P.O.Box 2345, Beijing 100023,China
Fax: +86-10-85381893
E-mail: wjg@wjgnet.com www.wjgnet.com

World J Gastroenterol 2003;9(12):2726-2731
World Journal of Gastroenterology
 ISSN 1007-9327

• BASIC RESEARCH •

Differentially expressed proteins of gamma-ray irradiated mouse intestinal epithelial cells by two-dimensional electrophoresis and MALDI-TOF mass spectrometry

Bo Zhang, Yong-Ping Su, Guo-Ping Ai, Xiao-Hong Liu, Feng-Chao Wang, Tian-Min Cheng

Bo Zhang, Yong-Ping Su, Guo-Ping Ai, Xiao-Hong Liu, Feng-Chao Wang, Tian-Min Cheng, Institute of Combined Injury of PLA, Third Military Medical University, Chongqing 400038, China
Supported by the National Natural Science Foundation of China, No.30230360
Correspondence to: Professor Yong-Ping Su, Institute of Combined Injury of PLA, Third Military Medical University, Gaotanyan Street 30, Chongqing 400038, China. mouse@mail.tmmu.com.cn
Telephone: +86-23-68752355 **Fax:** +86-23-68752279
Received: 2003-05-13 **Accepted:** 2003-06-12

Abstract

AIM: To identify the differentially expressed proteins involved in ionizing radiation in mice and to explore new ways for studying radiation-related proteins.

METHODS: Bal B/c mice grouped as sham-irradiation, 3 h and 72 h irradiation were exposed to 9.0Gy single dose of γ-irradiation. Intestinal epithelia were isolated from mice, and total proteins were extracted with urea containing solution. A series of methods were used, including two-dimensional electrophoresis, PDQuest 2-DE software analysis, peptide mass fingerprinting based on matrix-assisted laser desorption/ionization time of flight mass spectrometry (MALDI-TOF-MS) and SWISS-PROT database searching, to separate and identify the differential proteins. Western blotting and RT-PCR were used to validate the differentially expressed proteins.

RESULTS: Mouse intestine was severely damaged by 9.0 Gy γ-irradiation. Image analysis of two-dimensional gels revealed that averages of 638±39, 566±32 and 591±29 protein spots were detected in 3 groups, respectively, and the majority of these protein spots were matched. About 360 protein spots were matched between normal group and 3 h irradiation group, and the correlation coefficient was 0.78 by correlation analysis of gels. Also 312 protein spots matched between normal group and 72 h irradiation group, and 282 protein spots between 3 h and 72 h irradiation groups. Twenty-eight differential protein spots were isolated from gels, digested with trypsin, and measured with MALDI-TOF-MS. A total of 25 spots yielded good spectra, and 19 spots matched known proteins after database searching. These proteins were mainly involved in anti-oxidation, metabolism, signal transduction, and protein post-translational processes. Western-blotting confirmed that enolase was up-regulated by γ-irradiation. Up-regulation of peroxiredoxin I was verified by applying RT-PCR technique, but no change occurred in Q8VC72.

CONCLUSION: These differentially expressed proteins might play important roles when mouse intestine was severely injured by γ-irradiation. It is suggested that differential proteomic analysis may be a useful tool to study the proteins involved in radiation damage of mouse intestinal epithelia.

Zhang B, Su YP, Ai GP, Liu XH, Wang FC, Cheng TM. Differentially expressed proteins of gamma-ray irradiated mouse intestinal epithelial cells by two-dimensional electrophoresis and MALDI-TOF mass spectrometry. *World J Gastroenterol* 2003; 9(12): 2726-2731
http://www.wjgnet.com/1007-9327/9/2726.asp

INTRODUCTION

Since Wilkins and Williams first proposed the concept of "Proteome" in 1994[1], advances in the studies on proteome have made it possible to compare the total proteins of cells under different conditions on large scale. The proteomic strategy based on two-dimensional electrophoresis (2-DE) and mass spectrometry has been applied in a variety of studies[2,3].

Ionizing radiation is one of the main treatment modalities used in the management of pelvic cancer. Selective internal radiation therapy is a new method that can be used for patients given other routine therapies but without effects, and preoperative radiotherapy is effective and safe[4,5]. Although great success has been documented in cancer patients, certain side effects and complications have limited its applications in cancer radiotherapy. One of the major side effects of ionizing radiation is the depletion of normal cells along with cancer cells. For patients with pelvic cancer, a serious complication of radiotherapy is the radiation injury to small intestinal epithelium[6].

Small intestinal epithelium contains four major cell types: columnar cells, goblet cells, stem cells, and Paneth cells[7]. Intestinal stem cells, which are most sensitive to ionizing radiation, are located in the crypt portion of the intestine. The impact of ionizing radiation on intestinal stem cells can be detected at a dose as low as 0.05 Gy[8]. One of the early morphological changes that occur in mouse crypt cells upon treatment with ionizing radiation is the occurrence of apoptosis within 2-3 h after administration of the treatment. This apoptotic death can be visualized under both light and electron microscopy. Because of the emigration of crypt cells from the villi and the decreased proliferation of intestinal stem cells, the crypts become noticeably smaller 14-15 h after radiation[9]. The villous epithelial cells begin to decline from about the second day post radiation, and the villi become shorter. If a crypt contains viable clonogenic cells, the crypt begins to replenish its cellular population in the next few days.

Ionizing radiation can generate a series of biochemical events inside the cell. Free radicals produced from intercellular water interact with DNA and proteins, thus inducing inactivation of these macromolecules. It has been demonstrated that ionizing radiation can induce gene expression of intestinal epithelia[10,11]. As genes encode proteins, we can deduce that proteins of intestinal epithelia can be induced by ionizing radiation[12]. These proteins are associated with many important cellular processes including DNA repair, apoptosis, cell cycle control, and oxidative stress response[13,14]. With accumulating evidences in the literature that new proteins are implicated in

radiation response, the molecular mechanism underlying radiation response of the small intestine remains unknown. Our aim was to identify these proteins in the early stage of radiation injury. To achieve this purpose, we adopted comparative proteome approach to identify the mouse proteins whose expression was regulated by ionizing radiation. The proteomes of sham-irradiated mice were compared with those of irradiated mice 3 h and 72 h post-irradiation. The differentially displayed proteins were subjected to MALDI-TOF-MS to establish the identity. We also confirmed some differential proteins by Western blot and RT-PCR technique.

MATERIALS AND METHODS

Animal model and irradiation

A total of 15 male Bal b/c mice, 58-62 days of age, weighing 20-24 g, at the time of irradiation, were housed in conventional cages with free access to drinking water and standard chow. A pathogen-free environment with controlled humidity and temperature was maintained. These mice were randomly divided into 3 groups: one group received sham-irradiation (n=5), the other two groups received single dose of 9.0 Gy (n=5). The dose was chosen based on the data from our previous experiments. Whole-body irradiation was performed with a ^{60}Co-source at a dose rate of 0.78 Gy/min. The irradiated mice were killed 3 h and 72 h post-radiation, and intestines were removed and histological sections were made according to reference[15].

Isolation of mouse intestinal epithelia

Mouse intestinal epithelial cells were isolated according to the method described by Bjerknes[16] with slight modifications. In brief, animals were sacrificed, and the small intestine was removed and perfused with 30 ml of cold PBS. Then it was gently everted using a glass rod and flushed by PBS with its two ends enveloped. The swollen intestine was transferred to a flask, and immersed into warm PBSE solution (PBS containing EDTA 1 mmol/L), and shaken at 150 cycles per min. After shaken for 5 min, the intestine was transferred to another clean flask with warm PBSE solution, and vibrated for another 5 min. The shed intestinal epithelial cells were centrifuged at 500×g for 10 min, and prepared for protein extraction.

Protein extraction

The cell pellet harvested as described above was then washed in ice-cold PBS 3 times. Cells were resuspended in cold PBS, and counted. Total proteins were extracted from 10^7 cells with an appropriate volume (200 μl) of lysis buffer containing 7 mol/L urea, 2 mol/L thiourea, 65 mmol/L DTT, 2 % CHAPS, 2 mmol/L PMSF, 0.5 % IPG buffer, and protease inhibitor mixture. The extraction mixture was sonicated using a MSE 100 ultrasonic probe, and then centrifuged at 12 000×g for 20 min. After transferred to a clean tube, the supernatant was stored at -70 ℃ as aliquots. The protein concentration was determined using Bradford dye-binding assay with bovine serum albumin as the standard.

Two-dimensional electrophoresis

Two-dimensional electrophoresis was carried out by using the Mini-PROTEIN 2-D apparatus (Bio-Rad). For isoelectric focusing (IEF), precast IPG strips (Immobiline DryStrips, Amersham Pharmacia Biotech, Uppsala, Sweden) were used. Samples were applied via rehydration of IPG strips in sample solution for more than 12 h. Before application, the samples were diluted to a total volume of 350 μl with rehydration buffer (8 mol/L urea, 2 % CHAPS, 0.5 % IPG buffer, 0.3 % DTT, and a trace of bromophenol blue). Protein sample (1 000 μg) was loaded onto an 18 cm IPG strip (pH3-10, linear), and isoelectric focusing was run for 45 KVh at 20 ℃. To improve the sample entry, low voltage (100V) was applied for 2 h at the beginning. After IEF separation, the IPG strips were immediately equilibrated for 2×15 min with buffer (50 mmol/L Tris-HCl, pH6.8, 6 mol/L urea, 30 % glycerol, 2 % SDS, and a trace of bromophenol blue). DTT (2 %) was added in the first step, and iodoacetamide in the second step. For the second dimensional separation, the concentration of homogeneous SDS-polyacrylamide gels was 13 %. The proteins in the equilibrated strips were run at a current of 30 mA/strip for about 5 h until the bromophenol dye reached the bottom of the gels. Molecular mass marker was run on the same gel to determine the relative molecular masses of the proteins.

Image processing and analysis

After electrophoresis, the resolved proteins in 2-DE gels were fixed in ethanol/acetic acid/water (4/1/5) for at least 1 h, and then visualized by Coomassie blue R-250. The gels were scanned (Gel Doc 2000, Bio-Rad), and the images were processed with PDQuest software (Ver 7.0, Bio-Rad). To determine the variation, three gels were prepared for each sample. The computer analysis allowed automatic detection and quantification of protein spots, as well as matching between control gel and treatment. Protein spots that were new, absent, up- and down-regulated, were simultaneously displayed on the same image using the gels of sham-irradiated sample as the reference.

Protein identification by MALDI-TOF-MS

The differential protein spots were exactly excised from the gels. Gel pieces were destained with 50 % acetonitrile for several times until Coomassie blue was invisible. Then gel pieces were dried in a vacuum centrifuge. The shrinking gel pieces were re-swollen with 5 μl of protease solution (trypsin at 0.05 μg/μl in digestion buffer of 25 mmol/L NH4HCO3). Additional 50 μl of digestion buffer was added into the gel piece. Digestion was performed overnight at 37 ℃. Next, 50 μl of 5 % TFA solution was added to the gel piece, followed by incubation for 60 min at 42 ℃. The supernatant was collected and concentrated using ZipTip pipette tips (Millipore) according to the manufacturer' s instructions. The samples were mixed on the MALDI target with matrix DBA solution. Peptide mass maps were generated by applying Biosystems Voyager 6192 MALDI-TOF-Mass Spectrometry (ABI, USA). Database searching was performed using monoisotopic peptide masses obtained from MALDI-TOF-MS. The SWISS-PROT and TrEMBL database was searched with PeptIdent software (http://www.expasy.org/tools/pep-tident.html). Peptide masses were assumed to be monoisotopic masses and cystines were assumed to be iodoacetamided. The peptide mass tolerance was set to 0.2Da, and the maximum of missed cleavage site was set to 1. Species was set as mouse.

Immunoblotting

Total proteins were separated on 12 % SDS-polyacrylamide gel, and then transferred to nitrocellulose membranes. After blocked for 1 h in the Tris/NaCl (50 mmol/L Tris-HCl, 200 mmol/L NaCl, 0.05 % Tween-20, pH7.4) containing 2 % BSA, membranes were probed with the goat anti-mouse Enolase polyclonal antibody (Santa Cruz, USA). Immunoreactive bands were visualized with a solution containing 1 mg/ml DAB and 0.01 % H_2O_2.

Semi-quantitative RT-PCR

Total RNAs were isolated from mouse intestinal epithelia with

TriPure isolation reagent (Roche, USA) according to the manufacturer' s descriptions. Peroxiredoxin I, Q72VC8, and GAPDH transcripts were determined by reverse transcriptase-polymerase chain reaction (RT-PCR) with RNA PCR kit (Takara, China). The primers for peroxiredoxin I are 5' GTTCTCACGGCTCTTTCTGTTT-3' and 5' CTTCTGGCTGCTCAATGCTG-3', Q8VC72 5' TGGACAAAGCCTTCATAGCA-3' and 5' CCTGGCAGAAACCACAGTAGA-3', GAPDH 5' ACCACAGTCCATGCCATCAC-3' and 5' TCCACCACCCTGTTGCTGTA-3'. The amplification was performed with one denaturing cycle at 94 ℃ for 5 min, then 25-27 cycles at 94 ℃ for 40 s, at 55 ℃ for 40 s, at 72 ℃ for 40 s, and one final extension at 72 ℃ for 5 min. RT-PCR products were run on 1.2 % agarose gel.

RESULTS

Histological changes of mouse intestine after radiation

Mice after 9.0 Gy irradiation died within 4-6 days post-radiation, with the intestines severely injured. As shown in Figure 1, the histological changes after irradiation were in agreement with our previous experiments. Though the height of villi and crypts remained unchanged 3 h post-radiation, cell division of intestinal epithelia ceased, and the intestines were severely injured morphologically. Moreover, the height of intestinal crypts was obviously increased 72 h post-radiation, with villi decreased. This indicated that many survival epithelial cells proliferated.

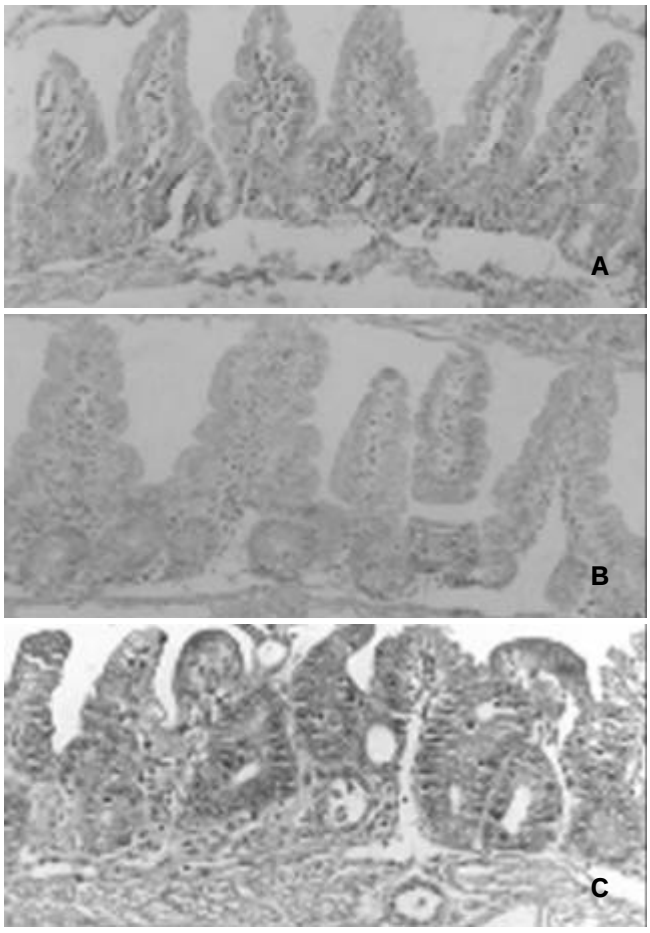

Figure 1 Histological changes in crypts following irradiation. A: Unirradiated controls (×100). B: 3 hours after a single dose of 9.0 Gy (×100). Villi and crypts remained unchanged, but cell division of intestinal epithelia ceased. C: 3 days after a single dose of 9.0 Gy (×100).

Two-dimensional electrophoresis and image analysis of mouse intestinal epithelia

To study the different proteins involved in ionizing radiation, we applied 2-DE to analyze the proteomic alteration of mouse intestinal epithelia. The 2-D patterns were highly reproducible since each experiment was performed in triplicate and produced similar results. Figure 2 showed the representative 2-D maps of the mouse intestinal epithelia. Image analysis of 2-D gels revealed that averages of 638±39, 566±32 and 591±29 protein spots were detected in 3 groups respectively, and the majority of these protein spots were matched. About 360 protein spots were matched between normal group and 3 h irradiation group, and the correlation coefficient was 0.78 by correlation analysis of gels. Three hundred and twelve protein spots were matched between normal group and 72 h irradiation group, and 282 protein spots between 3 h and 72 h irradiation groups. The unmatched spots represented those induced by irradiation as new or absent proteins, which were the main alteration of proteome.

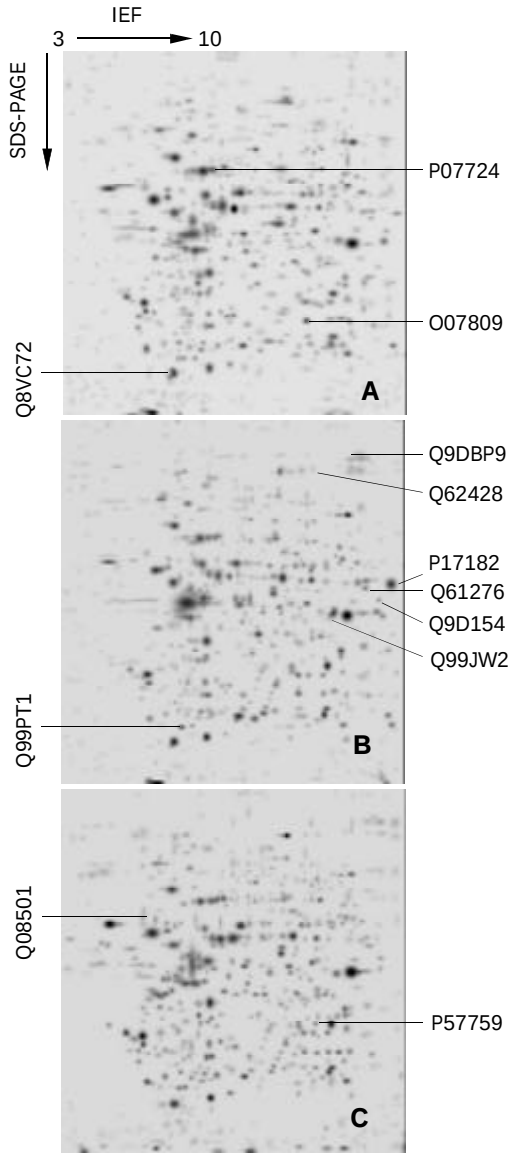

Figure 2 Two-dimensional electrophoresis maps. A: normal intestinal epithelial cells, B: 3 h irradiated epithelial cells, C: 72 h post-radiation. Number indicated proteins were summarized in Table 2.

Identification of proteins from 2-D gel spots

Out of a total of 28 spots excised from the gels, 25 spots yielded

nearly perfect MALDI spectra. A total of 19 spots were preliminarily identified by peptide mass fingerprinting. Figure 3 showed the typical peptide mass fingerprinting of Spot No. 11, whose peptides matched the mouse peroxiredoxin I. This spot was up-regulated by ionizing radiation. The identified proteins were summarized in Table 1. These proteins were involved in cellular process of anti-oxidation, metabolism, and protein post-translational processes. Other proteins, such as cellular structural proteins and hypothetic proteins derived from nucleic acid sequences, were also altered after irradiation. We also found, 6 spots with good MALDI spectra were returned with inconclusive match results, suggesting that they might be unknown proteins.

Induction of enolase by radiation

A protein spot was preliminarily identified as Enolase by

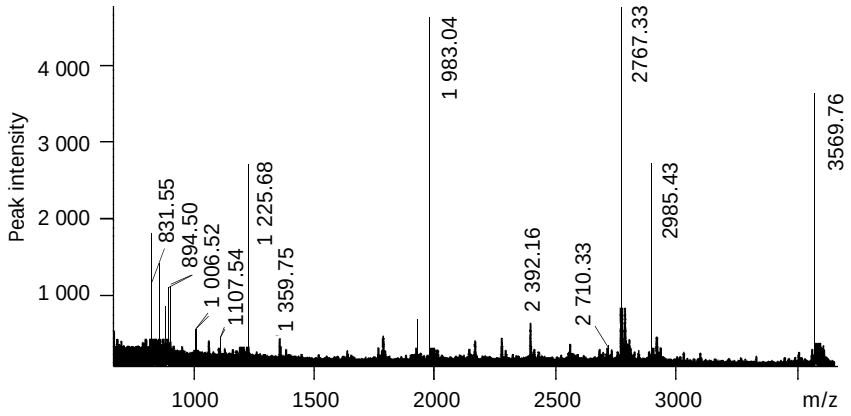

Figure 3 MALDI-TOF-MS spectrum of spot P35700 in 2-DE map. MS spectrum of peptide mixture was obtained from a typical in-gel digestion of the 2-DE separated protein.

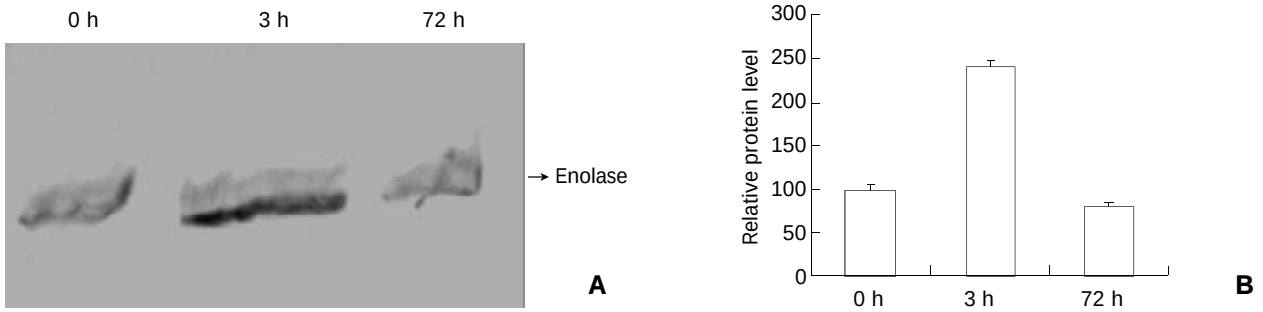

Figure 4 Western blot analysis of Enolase after radiation. A: Protein samples, obtained at indicated time after radiation, were separated by SDS-PAGE, and immunoblotted with corresponding antibody. Equal amounts of total proteins were applied to each lane. B: Relative protein level of Enolase was determined by quantitating the intensity of Enolase bands with a densitometer.

Table 1 Result of PeptIdent search of differential protein spots derived from BALB/c mice

Spot No.	Swiss-prot accession	Match rate	Theoretical pI/Mw	Sequence covered(%)	Protein name
N1	O08709	7/23	5.70/24871	28	Antioxidant protein 2
N2	P07724	17/39	5.53/65892	37.2	Serum albumin.
N3	Q8VC72	8/13	5.19/18573	58.9	Hypothetical 18.6 kDa protein
R1	Q9D154	8/28	5.85/42574	24.8	Serine protease inhibitor EIA
R2	Q99PT1	6/26	5.12/23391	27.0	Rho GDP-dissociation inhibitor 1
R3	Q61276	6/29	6.0/41693	26.0	A-X actin
R4	Q99JW2	9/31	5.9/45781	25.0	RIKEN cDNA 1110014J22 gene
R5	Q62428	15/27	5.72/92669	29.2	Villin 1
R6	Q9DBP9	12/38	6.2/105834	15.0	homolog to LON protease
R7	P17182	12/52	6.36/47009	36.7	Alpha enolase
R8	Q08501	5/20	5.00/68241	15.0	Prolactin receptor precursor
R9	P57759	5/17	5.74/25721	27.6	ERP29
R10	P19157	9/22	7.70/23609	48.8	Glutathione S-transferase P2
R11	Q9R0V2	6/40	4.86/21927	32.7	Truncated annexin IV.
R12	P35700	13/26	8.3/22177	33.0	Peroxiredoxin I
R13	P09041	5/33	6.6/44912	27.0	Phosphoglycerate kinase, testis specific
R14	P14701	5/15	4.80/19462	25.6	Translationally controlled tumor protein (TCTP)
R15	12847100[a]	8/14	6.9/28869	33.0	Aldo-keto reductase family 1, member A4
R16	P17182	13/35	6.36/47009	50.4	Alpha enolase

a: This protein was recorded in NCBI database.

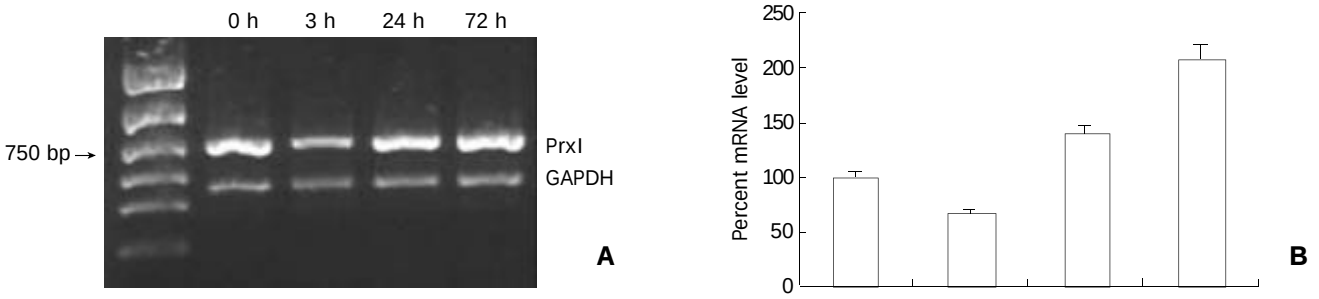

Figure 5 Semi-quantitative RT-PCR analysis of peroxiredoxin I. A: PCR product run on an agarose gel. The upper band represented peroxiredoxin I (750 bp), and the lower band represented GAPDH (450 bp). B: Relative abundance of the mRNA of peroxiredoxin I was normalized by GAPDH.

Figure 6 Semi-quantitative RT-PCR analysis of Q8VC72. RNA samples were prepared from mouse intestinal epithelia at indicated time. Left: The band represents Q8VC72 (461 bp). Right: The band represents GAPDH (450 bp). The expression of Q8VC72 remained unchanged after radiation.

MALDI-TOF-MS (Table 1), which was significantly increased in 3 h radiation group. Immunoblotting showed that Enolase was significantly up-regulated (2.1 fold more than the normal control, $P<0.01$, Figure 4). This confirmed our data of 2-D electrophoresis.

Induction of peroxiredoxin I and Q8VC72 by radiation

Semi-quantitative RT-PCR was used to detect the gene expression of peroxiredoxin I and Q8VC72. Total RNAs were isolated from normal and irradiated mouse intestine. The expression of peroxiredoxin I was markedly induced by radiation (Figure 5), using GAPDH as standard. However, the expression of Q8VC72 remained unchanged after radiation (Figure 6). This indicated that Q8VC72 might be a false-positive result.

DISCUSSION

A variety of techniques, including differential hybridization, differential display PCR, serial analysis of gene expression (SAGE), and gene array, have been used to identify the genes whose expression is selectively altered after radiation[17-19]. Recently, a new method termed gene trap strategy has also been used to predict radiation responsive genes[20]. All these methods are used to analyze the mRNA expression levels of radiation responsive genes. As mRNAs are easy to be degraded after transcription, and some are selectively translated, the quality and quantity of proteins do not correlate with that of mRNAs. Here, we applied 2-D electrophoresis to analyze the proteins involved in radiation response at protein level. As a large-scale screening of proteins, proteomics has been driven forward by the advent of the genome era[21], and it has become advantageous in analyzing total proteins of cells or tissues.

Many proteins have been demonstrated to be involved in radiation response among mammalians[22,23]. These proteins are associated with many important cellular processes such as DNA repair, apoptosis, signal transduction, and oxidative stress. Among the 19 preliminarily identified proteins, three spots belong to oxidative stress response proteins, i.e., peroxiredoxin I, glutathione S-transferase P2, and antioxidant protein 2. Radiation injuries are manifested as a result of increased production of reactive oxygen species (ROS), such as O_2, OH^-, and H_2O_2. These substances can induce the cellular antioxidant defense enzymes such as superoxide dismutase and glutathione peroxidase. In this study, peroxiredoxin I and glutathione S-transferase P2 were up-regulated by ionizing radiation, while antioxidant protein 2 was down-regulated. These proteins have been demonstrated to be involved in radiation[24-26]. Peroxiredoxin I is involved in the redox regulation of cells, such as reducing peroxides with reducing equivalents through the thioredoxin system but not from glutaredoxin. The function of glutathione S-transferase P2 has been found in conjugation of reduced glutathione to a large number of exogenous and endogenous hydrophobic electrophiles[27]. Antioxidant protein 2, also named 1-Cys peroxiredoxin, reduces H_2O_2 and phospholipid hydroperoxides. Our data confirmed the alteration of oxidative stress proteins with the exception of antioxidant protein 2. However, further studies will be performed to determine the mechanism as to why antixoxidant protein 2 does not play a critical role in ionizing radiation of small intestinal epithelial cells.

Using the proteomic strategy, we detected an interesting protein of ERP29 involved in ionizing radiation. ERP29 was first cloned from rat enamel cells, which had limited homology with protein disulfide isomerase and its cognate[28]. In this work, it was upregulated with ionizing radiation *in vivo*. ERP29 played an important role in the process of secretory proteins in the ER. Some researchers found that it played a role as a chaperone in protein folding[29,30]. The relationship between ERP29 and ionizing radiation has not yet been clarified, so it is worthy of further studying. In addition, some metabolic enzymes and hypothetical proteins, which were derived from nucleic acid sequences, were also found in this differential system. Their roles in ionizing radiation are unclear. Further researches are needed to draw precise conclusions. These data of hypothetical proteins suggest that these hypothetical proteins are expressed in intestinal epithelium indeed.

In brief, we compared the proteomics of mouse intestinal

epithelial cells with its irradiated counterparts *in vivo*. This strategy provides an efficient resolution to analyze radiation related proteins directly at protein level. The preliminarily identified proteins will be further studied in order to determine the cell signaling and molecular mechanisms of gene expression in radiation responses. This proteomic technique may contribute to the elucidation of the molecular mechanism of radiation damage, and can be applied in other research work as a useful tool.

REFERENCES

1 **Swinbanks D**. Government backs proteome proposal. *Nature* 1995; **378**: 653

2 **Xiong XD**, Xu LY, Shen ZY, Cai WJ, Luo JM, Han YL, Li EM. Identification of differentially expressed proteins between human esophageal immortalized and carcinomatous cell lines by two-dimensional electrophoresis and MALDI-TOF-mass spectrometry. *World J Gastroenterol* 2002; **8**: 777-781

3 **Fang DC**, Wang RQ, Yang SM, Yang JM, Liu HF, Peng GY, Xiao TL, Luo YH. Mutation and methylation of hMLH1 in gastric carcinomas with microsatellite instability. *World J Gastroenterol* 2003; **9**: 655-659

4 **Liu LX**, Zhang WH, Jiang HC. Current treatment for liver metastases from colorectal cancer. *World J Gastroenterol* 2003; **9**: 193-200

5 **Sun XN**, Yang QC, Hu JB. Pre-operative radiochemotherapy of locally advanced rectal cancer. *World J Gastroenterol* 2003; **9**: 717-720

6 **Smith DH**, DeCosse JJ. Radiation damage to the small intestine. *World J Surg* 1986; **10**: 189-194

7 **MacNaughton WK**. Review article: new insights into the pathogenesis of radiation- induced intestinal dysfunction. *Aliment Pharmacol Ther* 2000; **14**: 523-528

8 **Potten CS**, Owen G, Roberts SA. The temporal and spatial changes in cell proliferation within the irradiated crypts of the murine small intestine. *Int J Radiat Biol* 1990; **57**: 185-199

9 **Potten CS**. A comprehensive study of the radiobiological response of the murine (BDF1) small intestine. *Int J Radiat Biol* 1990; **58**: 925-973

10 **Somosy Z**, Horvath G, Telbisz A, Rez G, Palfia Z. Morphological aspects of ionizing radiation response of small intestine. *Micron* 2002; **33**: 167-178

11 **Hauer-Jensen M**, Richter KK, Wang J, Abe E, Sung CC, Hardin JW. Changes in transforming growth factor beta1 gene expression and immunoreactivity levels during development of chronic radiation enteropathy. *Radiat Res* 1998; **150**: 673-680

12 **Subramanian V**, Meyer B, Evans GS. The murine Cdx1 gene product localises to the proliferative compartment in the developing and regenerating intestinal epithelium. *Differentiation* 1998; **64**: 11-18

13 **Picard C**, Wysocki J, Fioramonti J, Griffiths NM. Intestinal and colonic motor alterations associated with irradiation-induced diarrhoea in rats. *Neurogastroenterol Motil* 2001; **13**: 19-26

14 **Dorr W**, Hendry JH. Consequential late effects in normal tissues. *Radiother Oncol* 2001; **61**: 223-231

15 **Jensen MH**, Sauer T, Devik F, Nygaard K. Late changes following single dose roentgen irradiation of rat small intestine. *Acta Radiol Oncol* 1983; **22**: 299-303

16 **Bjerknes M**, Cheng H. Methods for the isolation of intact epithelium from the mouse intestine. *Anat Rec* 1981; **199**: 565-574

17 **Hartmann KA**, Modlich O, Prisack HB, Gerlach B, Bojar H. Gene expression profiling of advanced head and neck squamous cell carcinomas and two squamous cell carcinoma cell lines under radio / chemotherapy using cDNA arrays. *Radiother Oncol* 2002; **63**: 309-320

18 **Amundson SA**, Bittner M, Meltzer P, Trent J, Fornace AJ Jr. Induction of gene expression as a monitor of exposure to ionizing radiation. *Radiat Res* 2001; **156**(5 Pt 2): 657-661

19 **Liu LX**, Jiang HC, Liu ZH, Zhou J, Zhang WH, Zhu AL, Wang XQ, Wu M. Integrin gene expression profiles of human hepatocellular carcinoma. *World J Gastroenterol* 2002; **8**: 631-637

20 **Vallis KA**, Chen Z, Stanford WL, Yu M, Hill RP, Bernstein A. Identification of radiation- responsive genes *in vitro* using a gene trap strategy predicts for modulation of expression by radiation *in vivo*. *Radiat Res* 2002; **157**: 8-18

21 **Yanagida M**. Functional proteomics; current achievements. *J Chromatogr B Analyt Technol Biomed Life Sci* 2002; **771**: 89-106

22 **Potten CS**, Booth C. The role of radiation-induced and spontaneous apoptosis in the homeostasis of the gastrointestinal epithelium: a brief review. *Comp Biochem Physiol B Biochem Mol Biol* 1997; **118**: 473-478

23 **Johnston MJ**, Robertson GM, Frizelle FA. Management of late complications of pelvic radiation in the rectum and anus: a review. *Dis Colon Rectum* 2003; **46**: 247-259

24 **Lee K**, Park JS, Kim YJ, Soo Lee YS, Sook Hwang TS, Kim DJ, Park EM, Park YM. Differential expression of Prx I and II in mouse testis and their up-regulation by radiation. *Biochem Biophys Res Commun* 2002; **296**: 337-342

25 **Mittal A**, Pathania V, Agrawala PK, Prasad J, Singh S, Goel HC. Influence of Podophyllum hexandrum on endogenous antioxidant defence system in mice: possible role in radioprotection. *J Ethnopharmacol* 2001; **76**: 253-262

26 **Lee YS**, Lee MJ, Lee M, Jang J. Susceptibility to the induction of glutathione S-transferase positive hepatic foci in offspring rats after gamma-ray exposure during gestation. *Oncol Rep* 2000; **7**: 387-390

27 **Strange RC**, Spiteri MA, Ramachandran S, Fryer AA. Glutathione-S-transferase family of enzymes. *Mutat Res* 2001; **482**: 21-26

28 **Hubbard MJ**, McHugh NJ, Carne DL. Isolation of ERp29, a novel endoplasmic reticulum protein, from rat enamel cells evidence for a unique role in secretory-protein synthesis. *Eur J Biochem* 2000; **267**: 1945-1957

29 **Sargsyan E**, Baryshev M, Szekely L, Sharipo A, Mkrtchian S. Identification of ERp29, an endoplasmic reticulum lumenal protein, as a new member of the thyroglobulin folding complex. *J Biol Chem* 2002; **277**: 17009-17015

30 **Kwon OY**, Park S, Lee W, You KH, Kim H, Shong M. TSH regulates a gene expression encoding ERp29, an endoplasmic reticulum stress protein, in the thyrocytes of FRTL-5 cells. *FEBS Lett* 2000; **475**: 27-30

Edited by Ma JY